Vol. 6, No. 3, 2015
ISSN 2233-4203/ e-ISSN 2093-8950
LETTER www.msletters.org | Mass Spectrometry Letters

Optimum Radius Size between Cylindrical Ion Trap and Quadrupole Ion Trap

Sarkhosh Seddighi Chaharborj,[1,2,3]* Seyyed Mahmod Sadat Kiai,[3] Norihan Md Arifin,[1] and Yousof Gheisari[2]

[1]*Department of Mathematics Faculty of Science, Universiti Purta Malaysia, 43400 UPM, Malaysia*
[2]*Department of Mathematics, Islamic Azad University, Bushehr Branch, Bushehr, Iran*
[3]*Plasma Physics and Nuclear Fusion Research school, Nuclear Science and Technology Research Institute (NSTRI), P.O. Box 14395-836, Tehran, Iran*

Received August 08, 2014; Revised October 06, 2014; Accepted October 06, 2014
First published on the web September 30, 2015; DOI: 10.5478/MSL.2015.6.3.59

Abstract: Quadrupole ion trap mass analyzer with a simplified geometry, namely, the cylindrical ion trap (CIT), has been shown to be well-suited using in miniature mass spectrometry and even in mass spectrometer arrays. Computation of stability regions is of particular importance in designing and assembling an ion trap. However, solving CIT equations are rather more difficult and complex than QIT equations, so, analytical and matrix methods have been widely used to calculate the stability regions. In this article we present the results of numerical simulations of the physical properties and the fractional mass resolutions $m/\Delta m$ of the confined ions in the first stability region was analyzed by the fifth order Runge-Kutta method (RKM5) at the optimum radius size for both ion traps. Because of similarity the both results, having determining the optimum radius, we can make much easier to design CIT. Also, the simulated results has been performed a high precision in the resolution of trapped ions at the optimum radius size.

Keywords: Quadrupole ion trap, cylindrical ion trap, optimum radius size, fifth order Runge Kutta method, stability regions, ion trajectory, fractional mass resolution

Introduction

Ion trap mass spectrometry has been developed through several stages to its present situation of relatively high performance and increasing popularity. Quadrupole ion trap (QIT), invented by Paul and Steinwedel,[1] has been widely applied to mass spectrometry,[2-11] ion cooling and spectroscopy,[12] frequency standards, quantum computing,[13] and so on. However, various geometries has been proposed and used for QIT.[14]

An ion trap mass spectrometer may incorporate a Penning trap,[15] Paul trap[16] or the Kingdon trap.[17] The Orbitrap, introduced in 2005, is based on the Kingdon trap.[18] Also, the cylindrical ion trap CIT has received much attention in a number of research groups because of several merits. The CIT is easier to fabricate than the Paul ion trap which has hyperbolic surfaces. In addition, the relatively simple and small sized CIT make it an ideal candidate for miniaturization. Experiments using a single miniature CIT showed acceptable resolution and sensitivity, and limited by the ion trapping capacity of the miniature device.[19-21]

With these interests, many groups such as Purdue University and Oak Ridge National Laboratory have researched on the applications of the CIT to miniaturize mass spectrometer.[22,23]

Electric field inside CIT

In CIT, the hyperbolic ring electrode,[24] as in Paul ion trap, is replaced by a simple cylinder and the two hyperbolic end-cap electrodes are replaced by two planar end-plate electrodes.[25] The potential difference applied to the electrodes[24-26] is:

$$\Psi(r,\theta,z)=\sum_i \frac{2\Psi_0}{m_i r_1}\frac{J_0(m_i r)}{J_1(m_i r_1)}\frac{ch(m_i z)}{ch(m_i z_1)}, \quad (1)$$

with

$$\Psi_0 = -(U_{dc} - V_{ac}\cos(\Omega t)) \quad (2)$$

Where, U_{dc} is a direct potential, V_{ac} is the zero to peak

*Reprint requests to Sarkhosh Seddighi Chaharborj
E-mail: sseddighi2007@yahoo.com

amplitude of the RF voltage, Ω is RF angular frequency, and z_1 expresses the distance from the center of the CIT to the end cap and r_1 the distance from the center of the CIT to the nearest ring surface. The electric field in a cylindrical coordinate (r,z,θ) inside the CIT can be written as follows:

$$(E_r, E_\theta, E_z) = -\nabla\, \Psi(r, \theta, z) \tag{3}$$

here, ∇ is gradient. From Eq.(3) (grad), the following is retrieved:

$$(E_r, E_\theta, E_z) = \begin{bmatrix} \sum_i \frac{2\Psi_0}{r_1} \cdot \frac{J_1(m_i r)}{J_1(m_i r_1)} \cdot \frac{ch(m_i z)}{ch(m_i z_1)} \\ 0 \\ -\sum_i \frac{2\Psi_0}{r_1} \cdot \frac{J_0(m_i r)}{J_1(m_i r_1)} \cdot \frac{sh(m_i z)}{ch(m_i z_1)} \end{bmatrix} \tag{4}$$

The equation of the motions[10,21,24,25] of the ion of mass m and e can be written as

$$\frac{d^2u}{d\xi^2} - (\alpha - 2\chi\cos 2\xi) \cdot \sum_i \frac{J_1(\lambda_i u)}{J_1(\lambda_i)} \cdot \frac{ch(\lambda_i v)}{ch\left(\lambda_i \frac{z_1}{r_1}\right)} = 0 \tag{5}$$

$$\frac{d^2v}{d\xi^2} - (\alpha - 2\chi\cos 2\xi) \cdot \sum \frac{J_0(\lambda_i u)}{J_1(\lambda_i)} \cdot \frac{sh(\lambda_i v)}{ch\left(\lambda_i \frac{z_1}{r_1}\right)} = 0 \tag{6}$$

and the following

$$r_1^2 = 2z_1^2, \xi = \frac{\Omega t}{2}, m_i r_1 = \lambda_i, \frac{r}{r_1} = u, \frac{z}{r_1} = v, \alpha = -8\frac{e}{m} \cdot \frac{U_{dc}}{r_1^2\Omega^2}, \chi = -4\frac{e}{m} \cdot \frac{V_{ac}}{r_1^2\Omega^2}$$

Where J_0 and J_1 are the Bessel functions of the first kind of order 0 and order 1, respectively, whereas ch is the hyperbolic cosine function, $m_i r$ is the roots of equation $J_0(m_i r) = 0$. To obtain λ_i's the Maple software was employed to find $J_0(\lambda_i) = 0$ roots. Eqs.(5) and (6) are coupled in u and v (respective r and z), and thus, can only be treated as a rough approximation.[21,25] Therefore, studies on CIT equations are more difficult and complex compared to QIT equations. As stated earlier, the optimum radius size between CIT and QIT helps us to study QIT instead of CIT.[27]

The motions of ion inside quadrupole ion trap

A hyperbolic geometry for the Paul ion trap was assumed;

$\left(\frac{z}{z_0}\right)^2 - \left(\frac{r}{r_0}\right)^2 = \pm 1$, and $r_0^2 = 2z_0^2$.

Here, z_0 is the distance from the center of the QIT to the end cap and r_0 is the distance from the center of the QIT to the nearest ring surface. In each of the perpendicular directions r and z, the ion motions of the ion of mass m and charge e[5,24,28,29] may be treated independently with the following substitutions:

$$\frac{d^2r}{d\xi^2} + (a_r - 2q_r\cos 2\xi)r = 0, \tag{7}$$

$$\frac{d^2z}{d\xi^2} + (a_z - 2q_z\cos 2\xi)z = 0, \tag{8}$$

$$\xi = \frac{\Omega t}{2}, a_z = -2a_r = -4\frac{e}{m} \times \frac{U_{dc}}{z_0^2\Omega^2}, q_z = -2q_r = -2\frac{e}{m} \times \frac{V_{ac}}{z_0^2\Omega^2}$$

CIT and QIT stability parameters

If the ions the same species are taken into consideration and the same potential amplitude and frequency, the following relations has been obtained:

$$\frac{\alpha}{a_z} = 2\frac{z_0^2}{r_1^2} \text{ and } \frac{\chi}{q_z} = 2\frac{z_0^2}{r_1^2}. \tag{9}$$

From Eq.(9) and $r_0^2 = 2z_0^2$ one can obtain

$$\alpha = a_z\left(\frac{r_0}{r_1}\right)^2 \text{ and } \chi = q_z\left(\frac{r_0}{r_1}\right)^2. \tag{10}$$

The optimum radius between cylindrical ion trap and quadrupole ion Trap

In some papers,[21,24] stability parameters have been used to determine the optimum radius size for cylindrical ion trap compared to the radius size for the quadrupole ion trap, as following:

(i) $\chi = q_z \Leftrightarrow r_1 = r_0 \Leftrightarrow z_1 = z_0$ (11)

(ii) $\chi = 2q_z \Leftrightarrow r_0 = \sqrt{2}r_1 \Leftrightarrow z_0 = \sqrt{2}z_1$ (12)

Eqs.(11) and (12) are from Refs,[21,24] respectively. In this study, Eqs.(5), (6) and Eqs.(7), (8) were used for the same propose to find optimum radius size for cylindrical ion trap compared to the radius size for quadrupole ion trap, as:

$$\frac{d^2u}{d\xi^2} - \sum_i (\alpha - 2\chi\cos 2\xi) \cdot \frac{J_1(\lambda_i u)}{J_1(\lambda_i)} \cdot \frac{ch(\lambda_i v)}{ch\left(\lambda_i \frac{z_1}{r_1}\right)} = \frac{d^2u'}{d\xi^2} - \left(\frac{1}{2}a_z - q_z\cos 2\xi\right)u' \tag{13}$$

$$\frac{d^2v}{d\xi^2} + \sum_i (\alpha - 2\chi\cos 2\xi) \cdot \frac{J_0(\lambda_i u)}{J_1(\lambda_i)} \cdot \frac{sh(\lambda_i v)}{ch\left(\lambda_i \frac{z_1}{r_1}\right)} = \frac{d^2v'}{d\xi^2} + (a_z - 2q_z\cos 2\xi)v', \tag{14}$$

with $u' = r/r_0$ and $v' = z/z_0$. Where α and χ are the trapping

parameters, which λ_i is the root of equation $J_0(m_i r_1)=0$. Eqs.(13) and (14) are true when (α,χ) and (a_z,q_z) vqlues belong to stability regions. In this case, $u=u(0)=c_1$, $v=v(0)=c_2$, $u'=u'(0)=c_3$, and $v'=v'(0)=c_4$ were assumed. Here, $u(0)$, $v(0)$, $u'(0)$, $v'(0)$ are the initial values for u, v, u' and v', respectively. Now, from Eqs.(13) and (14) with $d^2u/d\xi^2=d^2c_1/d\xi^2=0$, $d^2v/d\xi^2=d^2c_2/d\xi^2=0$, $d^2u'/d\xi^2=d^2c_3/d\xi^2=0$ and $d^2v'/d\xi^2=d^2c_4/d\xi^2=0$ the following can be obtained:

$$\sum_i(\alpha-2\chi\cos 2\xi)\cdot\frac{J_1(c_1\lambda_i)}{J_1(\lambda_i)}\cdot\frac{ch(c_2\lambda_i)}{ch\left(\lambda_i\frac{z_1}{r_1}\right)}=c_3\left(\frac{1}{2}a_z-q_z\cos 2\xi\right) \quad (15)$$

$$\sum_i(\alpha-2\chi\cos 2\xi)\cdot\frac{J_0(c_1\lambda_i)}{J_1(\lambda_i)}\cdot\frac{sh(c_2\lambda_i)}{ch\left(\lambda_i\frac{z_1}{r_1}\right)}=c_4(a_z-2q_z\cos 2\xi) \quad (16)$$

In adding Eqs.(15)and (16), we have:

$$(\alpha-2\chi\cos 2\xi)\sum_i\left[\frac{J_0(c_1\lambda_i)}{J_1(\lambda_i)}\cdot\frac{ch(c_2\lambda_i)}{ch\left(\lambda_i\frac{z_1}{r_1}\right)}+\frac{J_1(c_1\lambda_i)}{J_1(\lambda_i)}\cdot\frac{sh(c_2\lambda_i)}{ch\left(\lambda_i\frac{z_1}{r_1}\right)}\right], \quad (17)$$
$$=(a_z-2q_z\cos 2\xi)\cdot\left[c_4+\frac{1}{2}\times c_3\right]$$

After substituting α, χ, a_z and q_z we have,

$$\left(-8\frac{e}{m}\cdot\frac{U_{dc}}{r_1^2\Omega^2}+8\frac{e}{m}\cdot\frac{V_{ac}}{r_1^2\Omega^2}\cos 2\xi\right)$$

$$\sum_i\left[\frac{J_0(c_1\lambda_i)}{J_1(\lambda_i)}\cdot\frac{ch(c_2\lambda_i)}{ch\left(\lambda_i\frac{z_1}{r_1}\right)}+\frac{J_1(c_1\lambda_i)}{J_1(\lambda_i)}\cdot\frac{sh(c_2\lambda_i)}{ch\left(\lambda_i\frac{z_1}{r_1}\right)}\right] \quad (18)$$

$$=\left(-4\frac{e}{m}\times\frac{U_{dc}}{z_0^2\Omega^2}+4\frac{e}{m}\times\frac{V_{ac}}{z_0^2\Omega^2}\cos 2\xi\right)\cdot\left[c_4+\frac{1}{2}\times c_3\right],$$

with $r_1^2=2z_1^2$ and $r_0^2=2z_0^2$. Eq.(18) gives the optimum value of z_1 and z_0 for CIT and QIT with conditions $c_1=c_3$ and $c_2=c_4$. After substituting $\lambda_i', s, c_1=c_3=0.01$ and $c_2=c_4=0.01$; in Eq.(18) and by simplification, we have:

$$0.066\frac{e(-1.0U_{dc}+V_{ac}\cos(2.0\xi))}{mz_1^2\Omega^2} \quad (19)$$
$$=0.060\frac{e(-1.0U_{dc}+V_{ac}\cos(2.0\xi))}{mz_0^2\Omega^2}$$

Therefore, using the Maple software we will have,

$$z=1.04978z_0. \quad (20)$$

In Eq.(20), $z_1=1.04978z_0$ is the optimum radius size between the quadrupole and the cylindrical ion traps. For any initial conditions we can obtain same answer with Eq.(20) almost. This optimal radius size ($z_1=1.04978z_0$) is almost comparable with the optimal radius size in Eq.(11) ($z_1=z_0$) when $\chi=q_z$.[21,24] For the various u; v; r; z when (α, χ) and (a_z,q_z) belongs to the stability regions, we found almost the comparable optimum values equivalent to Eq. (20) was found. For example with $c_1=c_3=0.005$, $c_2=c_4=0.01$ and $c_1=c_3=0.05$, $c_2=c_4=0.01$, we have $z_1=1.4976z_0$ and $z_1=1.05024z_0$, respectively.

Numerical results

Stability regions

There are two stability parameters which control the ion motion for each dimension z ($z=u$ or $z=v$) and ($z=z$ or $z=r$), and a_z, q_z in the case of cylindrical and quadrupole ion traps,[24] respectively. In the plane (a_z, q_z) and for the z axis, the ion stable and unstable motions are determined by comparing the amplitude of the movement to one for various values of a_z, q_z.[26,30] To compute the accurate elements of the motion

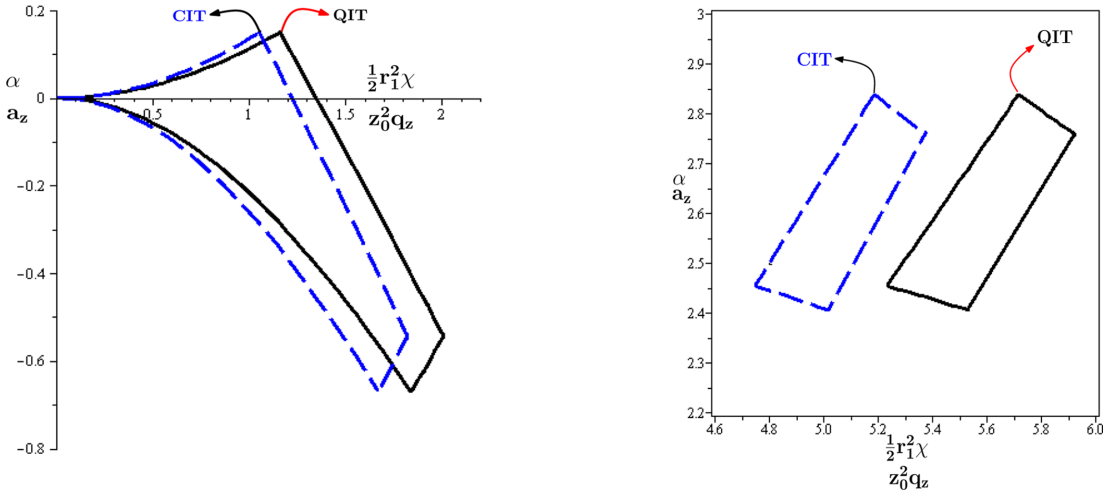

Figure 1. The first and second stability regions, black line (solid line): QIT with z_0= 0.82 cm and blue line (dash line): CIT with optimum radius size $z_1=1.04985z_0$ and $r_1^2=z_0^2$, (a): first stability region and (b): second stability region.

equations for the stability diagrams, we have used the fifth order Runge-Kutta numerical method with a 0.001 steps increment for Matlab software and scanning method.

Figure 1 (a) and (b) shows the calculated first and second stability regions for the quadrupole ion trap and cylindrical ion trap,[31] black line (solid line): QIT and blue line (dash line): CIT with optimum radius size $z_1 = 1.04978z_0$, (a): first stability region and (b): second stability region. Figure 1 shows that the apex of the stability parameters a_z stayed the same and the apex of the stability parameters q_z decrease for CIT to compare with QIT. Area of first stability regions for QIT and CIT are almost same, as 0.4136 and 0.4087, respectively. Figure 1 reveals almost a comparable stability diagram two methods.

Phase space ion trajectory

Figure 2 shows evolution of different values of the phase ion trajectory for ξ_0 with $\beta_z = 0.3 (z_0^2 q_z = 0.6089\ ,\ 1/2\ r_1^2\chi = 0.5525\ )$, red line : QIT with $z_0 = 0.82$ cm and blue line: CIT with the optimum radius size $z_1 = 1.04985z_0$, $r_1^2 = 2z_1^2$ and $z = r_1 v$.

The results illustrated in Figure 2 show that for the same equivalent operating point in two stability diagrams (having the same β_z), the associated modulated secular ion frequencies behavior are almost same for the quadrupole and cylindrical ion traps with the optimum radius size $z_1 = 1.04985z_0$. Table 1 presents the values of $z_0^2 q_z$ and $1/2\ r_1^2\chi$ for the quadrupole and cylindrical ion traps, when $a_z = 0$ and $\alpha = 0$ with the optimum radius size $z_1 = 1.04985z_0$, respectively for $\beta_z = 0.3.;0.6;0.9$. For the computations presented in Table 1, the following formulas were used:

$$\frac{a_z-\beta^2}{z_0^2 q_z} = \cfrac{1}{\cfrac{a_z-\beta^2}{z_0^2 q_z} - \cfrac{1}{\cfrac{a_z-(2+\beta)^2}{z_0^2 q_z} - \cfrac{1}{\cfrac{a_z-(4+\beta)^2}{z_0^2 q_z} - \cdots}}} + \cfrac{1}{\cfrac{a_z-\beta^2}{z_0^2 q_z} - \cfrac{1}{\cfrac{a_z-(\beta-2)^2}{z_0^2 q_z} - \cfrac{1}{\cfrac{a_z-(\beta-4)^2}{z_0^2 q_z} - \cdots}}} \tag{21}$$

and

$$\frac{a-\beta^2}{1/2\ r_1^2\chi} = \cfrac{1}{\cfrac{\alpha-\beta^2}{1/2\ r_1^2\chi} - \cfrac{1}{\cfrac{\alpha-(2+\beta)^2}{1/2\ r_1^2\chi} - \cfrac{1}{\cfrac{\alpha-(4+\beta)^2}{1/2\ r_1^2\chi} - \cdots}}} + \cfrac{1}{\cfrac{\alpha-\beta^2}{1/2\ r_1^2\chi} - \cfrac{1}{\cfrac{\alpha-(\beta-2)^2}{1/2\ r_1^2\chi} - \cfrac{1}{\cfrac{\alpha-(\beta-4)^2}{1/2\ r_1^2\chi} - \cdots}}} \tag{22}$$

for QIT and CIT, respectively. Hence, it is important to know that β_z point are the equivalent points; two operating points located in their corresponding stability diagram have the same β_z.[31] For the same $0 < \beta_z < 1$ we have, $0 < z_0^2 q_z < 1.35$ and $0 < 1/2 r_1^2\chi < 1.23$. Here, 1.35 and 1.23 are maximum values of stability diagrams for QIT and CIT when $a_z = 0$ and $\alpha = 0$ respectively. Therefore, for $\beta_z = 0$ we have $z_0^2 q_z = 0$, $1/2\ r_1^2\chi = 0$ and for $\beta_z = 1$ we have $z_0^2 q_z = 1.35$ and $1/2\ r_1^2\chi = 1.23$ for QIT and CIT, respectively. To compute Table 1, Maple software have been used.

The effect of optimum radius size on the mass resolution

The resolution of a quadrupole ion trap[9] and cylindrical ion trap mass spectrometry in general with optimum radius size $z_1 = 1.04985z_0$, is a function of the mechanical accuracy of the hyperboloid of the QIT Δr_0, and the cylindrical of the CIT Δr_1, and the stability performances of the electronics device such as, veriations in voltage amplitude ΔV, the rf frequency $\Delta\Omega$,[9] which tell us, how accurate is the form of the voltage signal.

Table 2 shows the values of $q_{z_{max}}$ and $V_{z_{max}}$ for the quadrupole ion trap and cylindrical ion trap with optimum radius size size $z_1 = 1.04985z_0$ in the first stability region

Table 1. The values of $z_0^2 q_z$ and $1/2\ r_1^2\chi$ for the quadrupole ion trap and cylindrical ion trap when $a_z = 0$ and $\alpha = 0$ with $z_0 = 0.82$ cm and optimum radius size $z_1 = 1.04985z_0$ and $r_1^2 = 2z_1^2$ for $\beta_z = 0.3, 0.6, 0.9$

β_z	$z_0^2 q_z$	$1/2\ r_1^2\chi$
	Quadrupole ion trap	Cylindrical ion trap
0.3	0.6089	0.5525
0.6	1.0893	0.9884
0.9	1.3335	1.2100

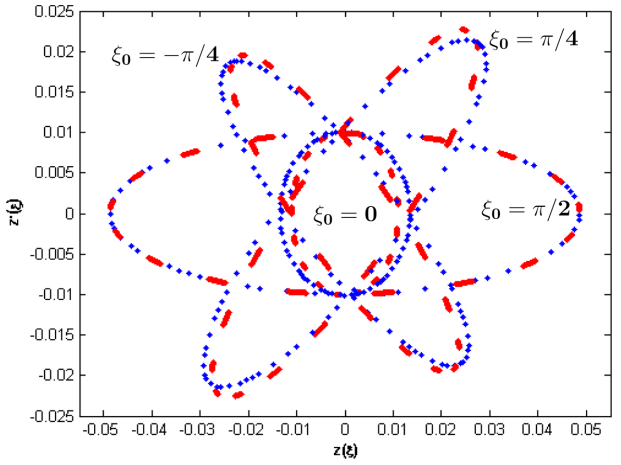

Figure 2. The evolution of the phase space ion trajectory for different values of the phase ζ_0 for $\beta_z = 0.3\ (z_0^2 q_z = 6.6089$, $1/2\ z_1^2\chi = 0.5525)$, red line: QIT with $z_0 = 0.82$ cm and blue line :CIT with optimum radius size $z_1 = 1.04985z_0$, $r_1^2 = 2z_1^2$ and $z = r_1 v$.

Table 2. The values of $q_{z_{\max}}$ and $V_{z_{\max}}$ for the quadrupole ion trap with optimum radius size $z_1 = 1.04985z_0$, respectively in the first stability region when $a_z = 0$

Ion Traps	$q_{z_{\max}}$	$V_{z_{\max}}$
QIT	2.01	5982.9425
CIT($z_1 = 1.04985z_0$)	1.65	16090.1156

when $a_z = 0$, respectively. The value of $V_{z_{\max}}$ has been obtained for ^{131}Xe with $\Omega = 2\Pi \times 1.05 \times 10^6$ rad/s, $U = 0$ V and $z_0 = 0.82$ cm in the first stability region when $a_z = 0$.

To obtain the values of Table 2 we suppose $V_{z_{\max}}$ as function of m, z_0^2, Ω^2, e for $m, z_1^2, \Omega^2, e, q_{z_{\max QIT}}/q_{z_{\max CIT}}$ for QIT and CIT with $z_1 = 1.04985z_0$, respectively as follows,

$$V_{z_{\max QIT}} \propto \frac{m z_0^2 \Omega^2}{2e} \tag{23}$$

$$V_{z_{\max CIT}} \propto \frac{m r_1^2 \Omega^2 q_{z_{\max QIT}}/q_{z_{\max CIT}}}{2e} \tag{24}$$

Now, we use Eqs.(23) and (24) to calculate $V_{z_{\max QIT}}$ and $V_{Z_{\max CIT}}$ for ^{131}Xe with $\Omega = 2\Pi \times 1.05 \times 10^6$ rad/s, $z_0 = 0.82$ cm and $z_1 = 1.04985z_0$ as follows,

$$V_{z_{\max QIT}} = \frac{(131/(6.022\times10^{26}))\times(0.82\times10^{-2})^2}{2\times1.602\times10^{-19}} \frac{\times(2\pi\times1.05\times10^6)^2}{2\times1.602\times10^{-19}} 5982.9425$$

$$V_{z_{\max CIT}} = \frac{(131/(6.022\times10^{26}))\times(\sqrt{2}\times1.04985\times0.82\times10^{-2})^2}{2\times1.602\times10^{-19}} \frac{\times(2\pi\times1.05\times10^6)^2\times(1.22)}{2\times1.602\times10^{-19}} 16090.1156$$

To derive a useful theoretical formula for the fractional resolution, one has to recall the stability parameters of the impulse excitation for the QIT and CIT with $z_1 = 1.04985z_0$, respectively as follows,

$$q_{z_{QIT}} = 4\frac{e}{m} \times \frac{V_{QIT}}{r_0^2\Omega^2}, \tag{25}$$

$$q_{z_{CIT}} = 4\frac{e}{m} \times \frac{V_{CIT}}{r_1^2\Omega^2} \tag{26}$$

By taking the partial derivatives with respect to the variables of the stability parameters $q_{z_{QIT}}$ for Eq.(25) and $q_{z_{CIT}}$ for Eq.(26), then the expression of the resolution Δm of the QIT and CIT, respectively are as follows,

$$\Delta m = \left(\frac{8eV_{QIT}}{r_0^3\Omega^2 q_{z_{QIT}}}\right)|\Delta r_0| + \left(\frac{4e}{r_0^2\Omega^2 q_{z_{QIT}}}\right)|\Delta V_{QIT}| + \left(\frac{8eV_{QIT}}{r_0^2\Omega^3 q_{z_{QIT}}}\right)|\Delta\Omega| \tag{27}$$

$$\Delta m = \left(\frac{8eV_{CIT}}{r_1^3\Omega^2 q_{z_{CIT}}}\right)|\Delta r_1| + \left(\frac{4e}{r_1^2\Omega^2 q_{z_{CIT}}}\right)|\Delta V_{CIT}| + \left(\frac{8eV_{CIT}}{r_1^2\Omega^3 q_{z_{CIT}}}\right)|\Delta\Omega| \tag{28}$$

Now to find the fractional resolution we have,

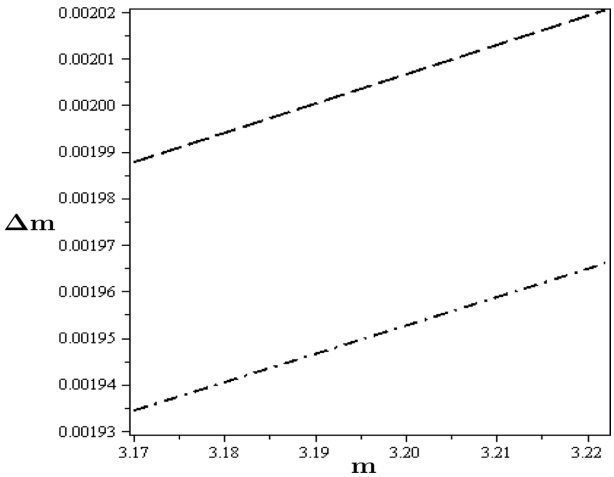

Figure 3. The resolution of Δm as function of ion mass m for ^{131}Xe with $\Omega = 2\Pi \times 1.05 \times 10^6$ rad/s, $z_0 = 0.82$ cm and $z_1 = 1.04985z_0$, dash line: for CIT and dash point line: for QIT.

$$\left(\frac{m}{\Delta m}\right)_{QIT} = \left\{\left|\frac{\Delta V_{QIT}}{V_{QIT}}\right| + 2\left|\frac{\Delta\Omega}{\Omega}\right| + 2\left|\frac{\Delta r_0}{r_0}\right|\right\}^{-1}, \tag{29}$$

$$\left(\frac{m}{\Delta m}\right)_{CIT} = \left\{\left|\frac{\Delta V_{CIT}}{V_{CIT}}\right| + 2\left|\frac{\Delta\Omega}{\Omega}\right| + 2\left|\frac{\Delta r_1}{r_1}\right|\right\}^{-1}, \tag{30}$$

Here Eqs.(29) and (30) are the fractional resolutions for QIT and CIT with optimum radius size $z_1 = 1.04985z_0$, respectively.

For the fractional mass resolution we have used the following uncertainties for the voltage, rf frequency and the geometry; $\Delta V / V = 10^{-15}$, $\Delta\Omega / \Omega = 10^{-7}$, $\Delta r_0 / r_0 = 3\times10^{-4}$. The fractional resolutions obtained are $m/\Delta m$ = 1638.806949;1638.398047 for QIT and CIT with optimum radius size $z_1 = 1.04985z_0$, respectively. When optimum radius size $z_1 = 1.04978z_0$ is applied, the rf only limited voltage is increased by the factor of approximately 2.6893, therefore, we have taken the voltage uncertainties as $\Delta V_{CIT}/V_{CIT} = 2.6893 \times 10^{-5}$. From Eqs.(29) and (30) we have $(m/\Delta m)_{\mathrm{QIT}}$ = 1638.8069 and $(m/\Delta m)_{\mathrm{CIT}}$ = 1598.6598 for QIT and CIT with optimum radius size $z_1 = 1.04985z_0$, recpectively. When these fractional resolutions are considered for the ^{131}Xe isotope mass $m = 3.18$, then, we have Δm = 0.001940436 and 0.001994156 for QIT and CIT with optimum radius size $z_1 = 1.04978z_0$, respectively. This means that, as the value of $m/\Delta m$ is decreased, the resolving power is increased due to increment in Δm. Experimentally, this means that the width of the mass signal spectra is better separated.

Discussion and conclusion

In this study, the behavior of the quadrupole and

cylindrical ion traps with the optimum radius has been considered. Also, it is shown that for the same equivalent operating point in two stability diagrams (i.e. having the same $\beta_z = 0.3$), the associated modulated secular ion frequencies behavior are almost the same with a suitable optimum radius size $z_1 = 1.04978 z_0$ with $r_1^2 = 2z_1^2$ and $r_0^2 = 2z_0^2$. This optimal radius size (z_1= 1.04978z_0) is almost comparable with the optimal radius size in Eq.(11) ($z_1 = z_0$) when x=q_z[22,25]

Table 1 also indicate that for the same equivalent operating point, almost a comparison physical size between two ion traps are shown; $z_1 = 1.04978 z_0 = 0.86$ cm and $z_0 = 0.82$ cm. The CIT has a smaller trapping parameter compared to QIT; for example for $\beta_z = 0.3$ we have $z_0^2 q_z = 0.6089$ and $1/2\ r_1^2 \chi = 0.5525$, a difference of 0.0564 higher for the QIT.

This difference in trapping parameters indicates that for the same rf and ion mass values, we need more confining voltage for CIT than QIT (see Table 2). So, higher fractional resolution can be obtained; higher separation confining voltages, especially for light isotopes[9,31] (see Figure 3).

References

1. Paul, W.; Steinwedel, H. *Z. Naturforsch.* **1953,** A8, 448.
2. March, R. E.; Todd J. F. J. *Modern Mass Spectrometry Series,* Vol. 1-3. CRC Press: Boca Ranton, **1995.**
3. Paul, W. *Rev. Mod. Phys.* **1990,** 62, 531
4. Major, F. G.; Gheorghe, V. N.; Werth, G. *Chraged particle traps,* Vol. 2. Springer, **2009**.
5. Kashanian, F.; Nouri, S.; Seddighi Chaharborj, S.; Mohd Rizam, A. B. *Int. J. Mass Spectrom.* **2011,** 303,199.
6. Sadat Kiai, S. M.; Andre, J.; Zerega, Y.; Brincourt, G.; Catella, R. *Int. J. Mass Spectrom. And ion processes.* **1991**, 107, 191.
7. Sadat Kiai, S. M.; Andre, J.; Zerega, Y.; Brincourt, G.; Catella, R. *Int. J. Mass Spectrom. And ion processes.* **1991**, 108, 65.
8. Sadat Kiai, S. M. *Int. J. Mass Spectrom.* **1999**, 188, 177.
9. Sadat Kiai, S. M.; Seddighi Chaharborj, S.; Abu Bakar, M. R.; Fudziah I. *J. Anal. At. Spectrom.* **2011,** 26, 2247
10. Seddighi Chaharborj, S.; Sadat Kiai, S. M. *J. Mass Spectrom.* **2010,** 45, 1111.
11. Seddighi Chaharborj, S.; Sadat Kiai, S. M.; Abu Bakar, M. R.; Ziaeian, I.; Fudziah, I. *Int. J. Mass spectrom.* **2012,** 39, 63.
12. Itano, W. M.; Heinzen, D. J.; Bollinger, J. J.; Wineland, D. J. *phys. Rev. A.* **1990,** 41, 2295.
13. Kielpinski, D.; Meyer, V.; Rowe, M. A.; Sackett, C. A.; Itano, W. M.; Monroe, C.; Wineland, D. J. *Science.* **2001,** 291, 1013.
14. Beaty, E. C. *J. Appl. Phys.* **1987,** 61, 2118.
15. Blaum, K. *physics Reports.* **2006,** 425, 1.
16. Douglas, D. J.; Frank, A. J.; Mao, D. M. *Mass Spectrometry Reviews.* **1923,** 21, 408.
17. Kingdon, K. H. *Physical Review.* **1923,** 21, 408.
18. Hu, Q. Z.; Noll, R. J.; Li, H. Y.;Makarov, A.; Hardman, M.; Cooks, R. G. *J. Mass spectrom.* **2005,** 40, 430.
19. Baranov, V. I. *J. Am. Soc. Mass Spectrom.* **2003,** 14, 818.
20. Badman, E. R. *Miniature cylindrical ion traps and arrays,* Ph. D. Thesis, Purdue University, **2001**.
21. Mather, R. E.; Waldren, R. M.; Todd, J. F. J.; March, R. E. *Int. Mass Spectrom. Ion Phys.* **1980,** 33, 201
22. Wells, J. M.; Badman, E. R.; Cooks, R. G. *Anal. Chem.* **1998,** 70, 438.
23. Kornienko, O.; Reilly, P. T. A.; Whitten W. B.; Ramsey, J. M. *Rev. Sci. Instrum.* **1999,** 70, 3907.
24. Benilan, M. N.; Audoin, C. *Int. J. Mass Spectrom. Ion Phys.* **1973,** 11, 421.
25. Bonner, R. F.; Fulford, J. E.; March, R. E.; Hamilton, G. F. *Int. Mass Spectrom. Ion Phys.* **1977,** 24, 255.
26. Lee, W. W.; Oh, C. H.; Kim, P. S.; Yang, M.; Song, K. *Int. Mass Spectrom.* **2003,** 230, 25.
27. Ziaeian, I.; Sadat Kiai, S. M.; Ellahi, M.; Sheibani, S.; Safarian, A. *Int. J. Mass Spectrom.* **2011,** 304, 25.
28. Schowartz, J. C.; Senko, M. W.; Syka, J. E. P. *JASMS.* **2002,** 13, 659.
29. March, R. E. *J. Mass Spectrom.* **1997,** 32, 351.
30. Noshad, H.; Kariman, B. S. *Int. J. Mass Spectrom.* **2011,** 308, 109.
31. Sadat Kiai, S. M.; Baradaran, M.; Adlparvar, S.; Khalaj, M. M. A.; Doroudi, A.; Nouri, S.; Shojai, A. A.; Abdollahzadeh, M.; Abbasi D, F.; Roshan, M. V.; BabazadehInt, A. R. *J. Mass Spectrom.* **2005,** 247, 61.